

Conversion of Laser Phase Noise to Amplitude Noise in an Optically Thick Vapor

10 March 2000

Prepared by

J. C. CAMPARO
Electronics and Photonics Laboratory
Laboratory Operations

Prepared for

SPACE AND MISSILE SYSTEMS CENTER
AIR FORCE MATERIEL COMMAND
2430 E. El Segundo Boulevard
Los Angeles Air Force Base, CA 90245

Engineering and Technology Group

DTIC QUALITY INSPECTED 3

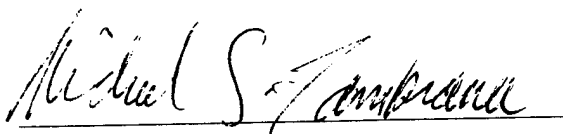
APPROVED FOR PUBLIC RELEASE;
DISTRIBUTION UNLIMITED

20000425 115

This report was submitted by The Aerospace Corporation, El Segundo, CA 90245-4691, under Contract No. F04701-93-C-0094 with the Space and Missile Systems Center, 2430 E. El Segundo Blvd., Los Angeles Air Force Base, CA 90245. It was reviewed and approved for The Aerospace Corporation by B. Jatuszliwer, Principal Director, Electronics and Photonics Laboratory. Michael Zambrana was the project officer for the Mission-Oriented Investigation and Experimentation (MOIE) program.

This report has been reviewed by the Public Affairs Office (PAS) and is releasable to the National Technical Information Service (NTIS). At NTIS, it will be available to the general public, including foreign nationals.

This technical report has been reviewed and is approved for publication. Publication of this report does not constitute Air Force approval of the report's findings or conclusions. It is published only for the exchange and stimulation of ideas.

A handwritten signature in dark ink, reading "Michael S. Zambrana". The signature is written in a cursive, flowing style. The first name "Michael" is written in a larger, more prominent script, followed by "S." and then "Zambrana". The signature is positioned above a horizontal line.

Michael Zambrana
SMC/AXE

REPORT DOCUMENTATION PAGEForm Approved
OMB No. 0704-0188

Public reporting burden for this collection of information is estimated to average 1 hour per response, including the time for reviewing instructions, searching existing data sources, gathering and maintaining the data needed, and completing and reviewing the collection of information. Send comments regarding this burden estimate or any other aspect of this collection of information, including suggestions for reducing this burden to Washington Headquarters Services, Directorate for Information Operations and Reports, 1215 Jefferson Davis Highway, Suite 1204, Arlington, VA 22202-4302, and to the Office of Management and Budget, Paperwork Reduction Project (0704-0188), Washington, DC 20503.

1. AGENCY USE ONLY (Leave blank)		2. REPORT DATE 10 March 2000	3. REPORT TYPE AND DATES COVERED	
4. TITLE AND SUBTITLE Conversion of Laser Phase Noise to Amplitude Noise in an Optically Thick Vapor			5. FUNDING NUMBERS F04701-93-C-0094	
6. AUTHOR(S) J. C. Camparo				
7. PERFORMING ORGANIZATION NAME(S) AND ADDRESS(ES) The Aerospace Corporation Technology Operations El Segundo, CA 90245-4691			8. PERFORMING ORGANIZATION REPORT NUMBER TR-96(8555)-2	
9. SPONSORING/MONITORING AGENCY NAME(S) AND ADDRESS(ES) Space and Missile Systems Center Air Force Materiel Command 2430 E. El Segundo Boulevard Los Angeles Air Force Base, CA 90245			10. SPONSORING/MONITORING AGENCY REPORT NUMBER SMC-TR-00-06	
11. SUPPLEMENTARY NOTES				
12a. DISTRIBUTION/AVAILABILITY STATEMENT Approved for public release; distribution unlimited			12b. DISTRIBUTION CODE	
13. ABSTRACT (Maximum 200 words) As laser light propagates through a resonant vapor, laser phase noise (PM) is converted to laser intensity noise (AM) because of the sensitivity of atomic coherence to laser phase fluctuations. In experiments reported here, it is shown that this PM-to-AM conversion process is highly efficient and can cause the relative intensity noise of transmitted diode laser light to be 1 to 2 orders of magnitude larger than the laser's intrinsic relative intensity noise. By use of a semi-classical description of the phenomenon, including the effect of optical pumping, reasonably good agreement between theory and experiment is obtained. The PM-to-AM conversion process discussed here has important consequences for atomic clock development, in which diode-laser optical pumping in thick alkali vapors holds the promise for orders-of-magnitude improvement in atomic clock performance.				
14. SUBJECT TERMS Atomic clock			15. NUMBER OF PAGES 10	
			16. PRICE CODE	
17. SECURITY CLASSIFICATION OF REPORT UNCLASSIFIED	18. SECURITY CLASSIFICATION OF THIS PAGE UNCLASSIFIED	19. SECURITY CLASSIFICATION OF ABSTRACT UNCLASSIFIED	20. LIMITATION OF ABSTRACT	

Acknowledgments

The author thanks R. Frueholz and B. Jaduszliwer for their support and encouragement during the course of this research, and S. B. Delcamp for help in performing the experiments. The author also thanks P. Lambropoulos for his collaboration on the general stochastic-field-atom interaction problem and for a critical reading of the manuscript. This research was supported by U.S. Air Force contract FO4701-93-C-0094.

Contents

1. INTRODUCTION	1
2. EXPERIMENTAL ARRANGEMENT	2
3. RADIATION TRAPPING	3
4. RELATIVE INTENSITY NOISE MEASUREMENTS	4
5. THEORY OF RELATIVE INTENSITY NOISE IN AN OPTICALLY THICK, OPTICALLY PUMPED VAPOR	5
REFERENCES AND NOTES	8

Figures

1a. Experimental arrangement for the study of laser PM-to-AM conversion in an atomic medium	2
1b. Schematic energy-level diagram of ^{87}Rb	2
2. Graph of the laser intensity transmitted through the resonance cell when the laser is tuned on resonance versus the incident laser intensity	3
3. Influence of radiation trapping on optical pumping	4
4a. RIN versus incident laser intensity	4
4b. RIN after passage through the resonance cell versus incident laser intensity with the laser tuned on resonance.....	4
5a. Example of computational laser transmitted intensity variations through 3 cm of a 50°C vapor for a laser with a 1-GHz linewidth and a RIN of 10^{-10}	7
6. Computational results for the RIN of laser light transmitted through a resonant rubidium vapor	8

Table

1. Parameters Used in the Computation of the Data Presented in Fig. 6	8
---	---

1. INTRODUCTION

Several years ago Yabuzaki *et al.*¹ found that when a phase fluctuating field passes through a resonant atomic or molecular medium the transmitted laser light displays enhanced intensity fluctuations. Moreover, the Fourier spectrum of those fluctuations maps out the medium's energy-level structure. Those authors pointed out that this phenomenon could be employed as a new kind of spectroscopy and explained their observations by noting that (in an optically thin vapor) a fluctuating laser's transmitted intensity is proportional to the product of the laser's electric field E and a randomly varying laser-induced polarization P . Because the polarization carries information on the medium's energy-level structure, so too will the transmitted intensity noise. Walser and Zoller² have since provided a careful analysis of this phenomenon in the regime of weak absorption, supporting the contention of Yabuzaki *et al.*, and McIntyre *et al.*³ have shown that this theoretical picture can provide good agreement between theory and experiment for optically thin vapors.

To date, most of the interest in the discovery of Yabuzaki *et al.* has centered on its spectroscopic applications. McLean *et al.*⁴ have demonstrated the utility of the phenomenon for the study of atmospheric oxygen, Vasavada *et al.*⁵ have shown that various detection schemes can highlight different atomic or molecular spectroscopic features, and Walser *et al.*⁶ have discussed its use in saturated absorption spectroscopy. However, the conversion of laser phase-modulation noise (PM) into amplitude-modulation noise (AM) has broader implications. In quantum electronic devices such as gas-cell atomic clocks⁷ the light intensity transmitted through a resonant atomic vapor provides the operative signal, and any process that decreases the signal-to-noise ratio of the device will degrade performance. Similarly, in spectroscopy experiments that take advantage of laser transmis-

sion through atomic or molecular vapors⁸ any increase in the noise of the transmitted laser intensity will degrade spectroscopic information. Unfortunately, for these broader implications of the PM-to-AM conversion process the assumption of optically thin vapors is often not justified, and it would be incorrect to extrapolate the thin vapor results into the optically thick vapor regime.

It is worth noting that this phenomenon has certain similarities to recent research that examined fluorescence intensity fluctuations induced by laser phase noise.⁹ However, whereas the fluorescence variations arise from phase-induced fluctuations in atomic population, the transmitted intensity variations under discussion here arise from phase-induced fluctuations in atomic coherence. Moreover, measurements of fluorescence intensity fluctuations have taken place in atomic beams, precluding a study of the phenomenon in an optically thick medium.

The physical origin of the PM-to-AM conversion process can be described semiclassically by use of Maxwell's equations. These yield in a standard fashion the electric field amplitude variation in a dielectric medium¹⁰:

$$\frac{\partial E}{\partial z} + \frac{1}{v} \frac{\partial E}{\partial t} = -\frac{2\pi k E}{n^2} |\chi''(z, E)|, \quad (1)$$

where k is the wave vector in the medium, n is the index of refraction, v is the phase velocity, and χ'' is the imaginary component of the electric susceptibility that in general will depend on E . If the stochastic and deterministic variations in E are slow compared with the time that it takes a wave front to propagate through the medium, then the time derivative in Eq. (1) can be ignored and an attenuation equation for the electric field amplitude can be obtained¹¹:

$$E(z) = E_0 \exp \left[-\frac{2\pi k}{n^2} \int_0^z |\chi''(z', E)| dz' \right]. \quad (2)$$

Laser phase fluctuations induce stochastic variations in χ'' , which in turn result in stochastic variations of the laser's electric field amplitude in the vapor. Thus, as the laser propagates through the medium, the atomic or molecular system converts the laser's phase fluctuations into laser intensity fluctuations.¹² For an optically thin vapor χ'' will be small and approximately constant over the length of the vapor, so expanding the exponential of Eq. (2) to first order yields

$$I(z) \sim |E(z)|^2 \cong |E_0|^2 - \frac{4\pi k}{n^2} E_0 P_z, \quad (3)$$

which clearly displays the PM-to-AM conversion process as a heterodyne signal between the laser's electric field and the vapor's induced polarization P , as noted by Yabuzaki *et al.*¹ However, in the general case χ'' will be neither small nor constant, and its stochastic variations will have an exponential, rather than a linear, influence on the transmitted laser electric field. This complication to the problem is more than academic, as devices such as gas-cell atomic clocks employ optically thick vapors with a spatially varying susceptibility as a consequence of optical pumping and atomic diffusion. Moreover, in these devices there is mixed collisional and Doppler broadening of the optical transition, which further complicates an understanding of PM-to-AM conversion.

In Section 2 the experimental arrangement is described, along with results related to optical pumping in an optically thick alkali vapor. Of particular note is the observation that the degree of optical pumping has a strong dependence on alkali density that is not easily explained as a consequence of spin exchange. In Section 3 it is argued that this alkali density dependence is a consequence of radiation trapping, even though the alkali vapor was in the presence of a 10-Torr N_2 buffer gas. In Section 4 the experimental results of PM-to-AM conversion are presented, and in Section 5 a semiclassical theory of the phenomenon is described and shown to be in reasonably good agreement with the experimental findings. Specifically, experiment and theory show that (1) the PM-to-AM conversion process increases the relative intensity noise (RIN) of transmitted diode-laser light by orders of magnitude in an optically thick vapor, (2) the enhancement of the RIN is a function of laser intensity, so there is little if any PM-to-AM conversion when efficient optical pumping reduces the number of atoms in the absorbing state, and (3) the enhancement of the RIN is a white-noise process at low Fourier frequencies (i.e., less than 25 kHz). Additionally, based on the discussion in Section 3, it is hypothesized that the PM-to-AM conversion process's extreme sensitivity to alkali density is a consequence of the relationship between radiation trapping and optical pumping in thick vapors.

2. EXPERIMENTAL ARRANGEMENT

Figure 1 shows a block diagram of the experimental arrangement. A Mitsubishi TJS¹³ AlGaAs diode laser (ML4102) was tuned near the Rb D_1 ($5^2P_{1/2} \rightarrow 5^2S_{1/2}$) transition at 794.7 nm and allowed to pass through a ^{87}Rb vapor contained within a Pyrex resonance cell.¹⁴

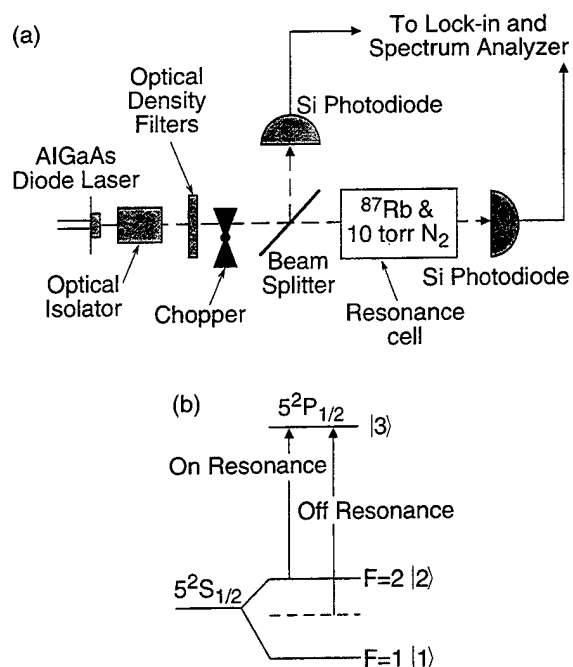


Fig. 1. (a) Experimental arrangement for the study of laser PM-to-AM conversion in an atomic medium. (b) Schematic energy-level diagram of ^{87}Rb . In the text, on resonance refers to the $5^2P_{1/2} \rightarrow 5^2S_{1/2}(F=2)$ transition, and off resonance refers to tuning the laser midway between the two ground-state hyperfine sublevel transitions to the $5^2P_{1/2}$ excited state. In the theoretical model the $5^2S_{1/2}(F=1)$, $5^2S_{1/2}(F=2)$, and $5^2P_{1/2}$ states are labeled |1>, |2>, and |3>, respectively.

The laser's linewidth was 60 MHz (FWHM), and it operated at an injection current of 1.3 times the threshold current, producing an output power of a few milliwatts. The laser beam was collimated and had an elliptical cross section with an area of $\sim 0.14 \text{ cm}^2$; 10 Torr of N_2 was also contained in the resonance cell as a buffer gas for efficient optical pumping.¹⁵ Basically, the N_2 served two purposes: It limited the rate of diffusion to the resonance cell walls where hyperfine polarization is destroyed [i.e., with respect to Fig. 1(a), |2>–|1> population imbalance], and it quenched atomic fluorescence, which can act as a depolarizing mechanism if it is reabsorbed by the atoms in the vapor. The resonance cell was heated by braided wire and centrally placed in a Helmholtz coil pair that produced a magnetic field of $\sim 300 \text{ mG}$ along the laser beam's propagation direction. The resonance cell was cylindrical, with a length L of 3.5 cm and a diameter of 2.5 cm, and for the experiments the resonance cell temperature varied between 30 and 45 °C. The Doppler-broadened linewidth was $\sim 510 \text{ MHz}$ and, when combined with the N_2 pressure-broadening contribution,¹⁶ produced a 619-MHz total linewidth for the optical transition.¹⁷ Resonance cell temperature, however, was not a good indicator of alkali vapor density. Because of the small amount of isotopically enriched ^{87}Rb in our resonance cell, the alkali vapor was not always saturated. Consequently, the optical depth τ_d of the vapor was measured by means of the relative absorption of laser light [i.e., by use of Beer's law,¹⁸ $\tau_d^{-1} = L^{-1} \ln(I_{\text{off}}/I_{\text{on}})$], where the subscripts refer to the laser tuned either off or on resonance, as illustrated in Fig. 1]. For the measurements of

τ_d an optical density filter of 4.0 was placed in the laser beam path to prevent optical pumping, and measurements spaced over several days at various temperatures were self-consistent.

Before entering the resonance cell the laser intensity was measured with a silicon photodiode, and after passing through the resonance cell the laser intensity was measured with an identical photodiode. An optical isolator, providing at least 36-dB isolation, prevented optical feedback from perturbing the laser characteristics, and the laser intensity could be attenuated by optical density filters placed in the laser beam path. Two sets of measurements were performed for each detector. The light beam was chopped and the average laser intensity $\langle I \rangle$ was measured with a lock-in amplifier. Then the chopper was stopped, and the intensity noise δI in a 1-Hz bandwidth at 209 Hz was measured with a spectrum analyzer that had a 25-kHz bandwidth. The laser RIN was defined as the ratio of δI to $\langle I \rangle$, and in all measurements δI was significantly larger than the photodetector's dark noise. (This definition of RIN is essentially the square root of that typically found in the diode-laser literature.) It should be noted for future reference that the spectrum of laser intensity noise was flat over the spectrum analyzer bandwidth for both photodetectors under all experimental conditions.

Figure 2 is a plot of the transmitted laser intensity $\langle I \rangle_{\text{trans}}$ versus the incident laser intensity $\langle I \rangle_{\text{inc}}$. For an optically thin vapor or exponential attenuation within the vapor, $\log(\langle I \rangle_{\text{trans}})$ will depend linearly on $\log(\langle I \rangle_{\text{inc}})$. As the figure shows, $\log(\langle I \rangle_{\text{trans}})$ displays a linear dependence on $\log(\langle I \rangle_{\text{inc}})$ for τ_d equal to 1.72 and 1.31 cm. Qualitatively we can explain these observations by noting that for $\tau_d = 1.31$ cm the resonant light was strongly absorbed by the vapor. Consequently, optical pumping was inefficient over the resonance cell volume, and exponential attenuation was operative. Alternatively, for $\tau_d = 1.72$ cm and the range of intensities investigated here there was more-efficient optical pumping over the resonance cell volume. Because optical pumping decreases the fraction of atoms in the absorbing state, the vapor

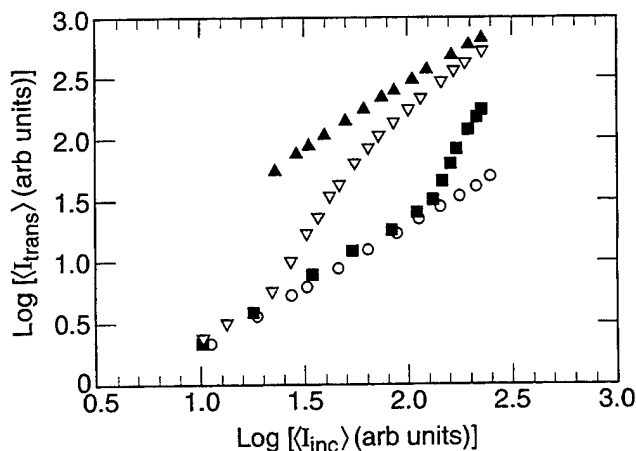


Fig. 2. Graph of the laser intensity transmitted through the resonance cell when the laser is tuned on resonance versus the incident laser intensity: filled triangles, $\tau_d = 1.72$ cm; open, inverted triangles, $\tau_d = 1.35$ cm; squares, $\tau_d = 1.33$ cm; circles, $\tau_d = 1.31$ cm.

acted as if it were optically thin. A similar change in a vapor's transmission characteristics was observed by Bhaskar *et al.*¹⁹, fluorescent wave fronts were found to propagate through an optically dense sodium vapor as laser optical pumping decreased the number density of absorbing atoms in the laser beam path. For values of τ_d equal to 1.33 and 1.35 cm, although optical pumping was inefficient at low light intensities it was reasonably efficient at high light intensities. Thus there is a transition in the dependence of $\log(\langle I \rangle_{\text{trans}})$ on $\log(\langle I \rangle_{\text{inc}})$ from a linearity that is due to exponential attenuation to a linearity associated with an optically thin vapor. As might be expected, the intensity where this transition takes place is higher for the vapor with the lower value of τ_d . Specifically, for $\tau_d = 1.35$ cm the transition occurs at $\log(\langle I \rangle_{\text{inc}}) \approx 1.4$, whereas for $\tau_d = 1.33$ cm the transition occurs at $\log(\langle I \rangle_{\text{inc}}) \approx 2.2$. As is discussed more fully in Section 3, it is believed that the extreme sensitivity of this transition intensity to optical depth is a consequence of radiation trapping.²⁰ Spin exchange¹⁵ is an unlikely mechanism to explain the effect, because the alkali density and hence the spin-exchange rate changed only by $\sim 2\%$ (i.e., $\tau_d = 1.35$ cm to $\tau_d = 1.33$ cm), yet the transition intensity changed by 145%.

3. RADIATION TRAPPING

As shown in Fig. 1(b), when the laser is tuned on resonance and radiation trapping is operative the reabsorption of fluorescent photons corresponding to the $|3\rangle \rightarrow |1\rangle$ transition will compete with the optical pumping process and inhibit the transfer of atomic population from $|2\rangle$ to $|1\rangle$. The rate of fluorescent photon reabsorption increases with alkali density and laser intensity. Consequently, for a significant reduction of population in the absorbing state to be achieved, a slight increase in alkali density could require a large increase in the optical pumping rate (i.e., laser intensity) to overcome the deleterious effects of radiation trapping. It is to be noted that, even though the 10 Torr of N_2 in the resonance cell provided for efficient quenching of the excited state (the $5^2P_{1/2}$ quenching rate was approximately three times faster than the fluorescent decay rate²¹), alkali fluorescence was nonetheless visible to the eye when the cell was observed with the aid of an infrared viewer. Moreover, previous experiments performed in our laboratory have indicated that N_2 buffer gas, even at a pressure of several Torr, is not always sufficient to eliminate completely the effects of radiation trapping in optical pumping experiments with alkali vapors.²² In this section a brief discussion of the role of radiation trapping in the experiment is presented and shown to explain qualitatively the appearance of Fig. 2.

As radiation trapping in multilevel systems is an area of research interest at present and is a difficult theoretical problem,²³ we crudely account for the influence of radiation trapping in our experiments by defining a probability p that a fluorescent photon is reabsorbed by the alkali vapor. The following set of rate equations that describe the optical pumping process can then be obtained:

$$\dot{\sigma}_1 = \frac{A}{2} \sigma_3 - \gamma_{\text{hfs}}(\sigma_1 - \sigma_2) - \frac{pA}{2} \sigma_3 \sigma_1, \quad (4a)$$

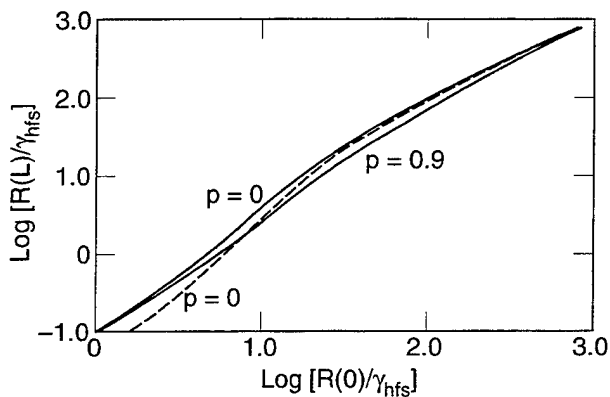


Fig. 3. Influence of radiation trapping on optical pumping: solid curves, $\tau_d = 1$ cm; dashed curve, $\tau_d = 0.8$ cm.

$$\dot{\sigma}_2 = -R\sigma_2 + \frac{A}{2}\sigma_3 + \gamma_{\text{hfs}}(\sigma_1 - \sigma_2) - \frac{pA}{2}\sigma_3\sigma_2, \quad (4b)$$

$$\dot{\sigma}_3 = R\sigma_2 - A\sigma_3 + \frac{pA}{2}\sigma_3(\sigma_1 + \sigma_2). \quad (4c)$$

Here A is the $5^2P_{1/2} \rightarrow 5^2S_{1/2}$ fluorescent decay rate, γ_{hfs} is the hyperfine polarization collisional relaxation rate, R is the excitation rate of $|2\rangle$, and $\sigma_i \equiv \sigma_{ii}$ is the population in $|i\rangle$. If R is much less than A , then $\sigma_1 + \sigma_2 \approx 1$, and Eqs. (4) can easily be solved in steady state to yield

$$\sigma_2 = -\left[\frac{(1-p)}{2p} + \frac{(2-p)\gamma_{\text{hfs}}}{pR}\right] + \left\{\left[\frac{(1-p)}{2p} + \frac{(2-p)\gamma_{\text{hfs}}}{pR}\right]^2 + \frac{(2-p)\gamma_{\text{hfs}}}{pR}\right\}^{1/2}. \quad (5)$$

Then, employing a Beer's law formula for the intensity of light transmitted through a vapor of length L results in

$$\frac{R(z + \delta z)}{\gamma_{\text{hfs}}} = \frac{R(z)}{\gamma_{\text{hfs}}} \left[1 - \sigma_2(z) \left(\frac{\delta z}{\tau_d}\right)\right]. \quad (6)$$

Using Eq. (5), we can solve Eq. (6) iteratively to determine the relative intensity at the exit of the vapor, $R(L)/\gamma_{\text{hfs}}$, for different values of the optical depth and probability of radiation trapping.

An example of this calculation is shown in Fig. 3 for $L = 5$ cm, where the relative intensity at the exit of the vapor is plotted against the relative input intensity, $R(0)/\gamma_{\text{hfs}}$. Three curves are shown: The two solid curves correspond to $\tau_d = 1$ cm with p equal to 0 or 0.9 and the dashed curve corresponds to $\tau_d = 0.8$ cm and $p = 0$. An important point to note from the figure is that, in the regime of $R(0)$ small, any significant decrease in τ_d reduces $R(L)$ for a fixed value of $R(0)$. Note, however, from Fig. 2(b) that in the regime of weak fields [i.e., $\log(\langle I_{\text{inc}} \rangle) \approx 1$], for a fixed incident laser intensity the optical depths of 1.31, 1.33, and 1.35 cm all yield the same value of $\log(\langle I_{\text{trans}} \rangle)$, consistent with the fact that these optical depths are close in value. Consequently it is difficult to rationalize the change in the transition intensity with an error in the optical depth measurements. Note, however, that on a qualitative level the data of Fig. 2 are

consistent with those of Fig. 3 (compare the two solid curves) under the assumption that a small change in alkali density can alter (perhaps significantly) the effects of radiation trapping.

Of course, one should not take this section's model of radiation trapping too far in explaining the experimental observations. At present little is known of the role of radiation trapping in optical pumping experiments,²⁴ and so by necessity the model discussed here was quite crude: neither geometrical effects nor Doppler distributions were discussed. With that said, however, it seems clear that, even in the presence of 10-Torr N_2 , radiation trapping plays an important role in the optical pumping of an optically thick alkali vapor.

4. RELATIVE INTENSITY NOISE MEASUREMENTS

Figure 4(a) shows the RIN of the diode laser before the laser beam enters the resonance cell (filled symbols) and also after it has passed through the resonance cell but

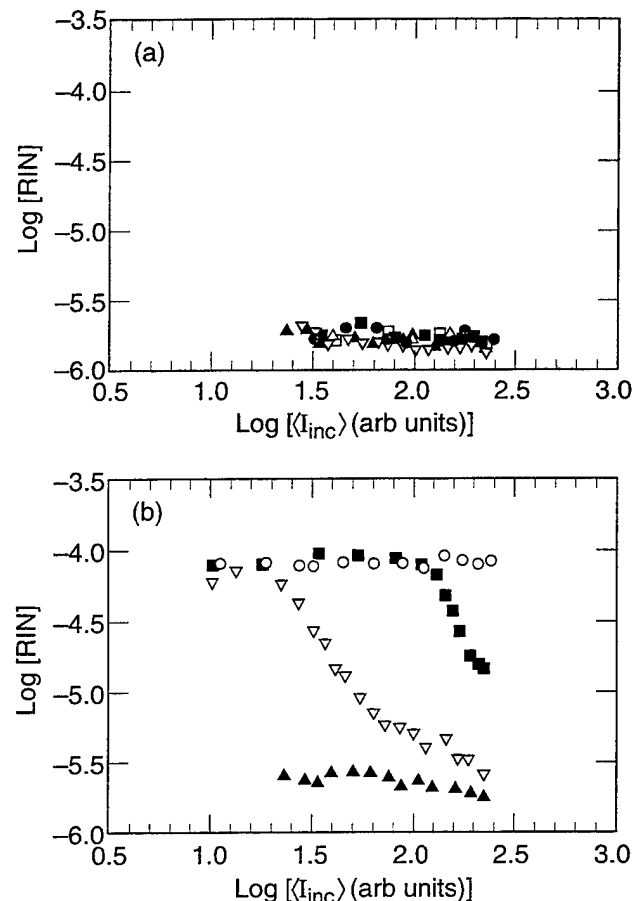


Fig. 4. (a) RIN versus incident laser intensity: filled symbols, measurements before the laser enters the resonance cell; open symbols, measurements made after passage of the laser through the resonance cell but tuned off resonance. Triangles, $\tau_d = 1.72$ cm; inverted triangles, $\tau_d = 1.35$ cm; squares, $\tau_d = 1.33$ cm; circles, $\tau_d = 1.31$ cm. (b) RIN after passage through the resonance cell versus incident laser intensity with the laser tuned on resonance. Symbols correspond to the values of τ_d as in (a).

tuned off resonance (open symbols). The various symbols correspond to experiments with different values of τ_d . As might be expected, the intrinsic RIN of the laser measured by the two photodetectors was essentially the same and yields a value of $\sim 1.7 \times 10^{-6}$. Further, this RIN value is independent of the laser intensity attenuated by the optical density filters. It should be noted that the measured RIN value is somewhat large, as CSP¹³ diode lasers typically have an intrinsic RIN roughly an order of magnitude smaller at our injection current level.²⁵ Moreover, at low Fourier frequencies the intensity noise of a diode laser is typically dominated by flicker ($1/f$) noise rather than by white noise.²⁶ Thus the source of our diode laser's intrinsic intensity noise might not be within the laser but might be associated with the laser electronics. Nevertheless, whatever its source, as is shown below, the laser's intrinsic intensity noise is insignificant compared with the intensity noise that appears in the transmitted signal after the laser has resonantly interacted with the atomic medium.

The RIN of the diode laser after propagation through the resonant atomic medium is shown in Fig. 4(b), and the most striking feature of the figure is the dramatic increase in RIN under certain experimental conditions (i.e., $\text{RIN}_{\text{trans}} \sim 8.0 \times 10^{-5}$ compared with $\text{RIN}_{\text{inc}} \sim 1.7 \times 10^{-6}$). For $\tau_d = 1.31$ cm, where optical pumping was inefficient, the enhancement of RIN is constant over the range of incident laser intensities investigated, whereas for $\tau_d = 1.72$ cm, where optical pumping was fairly efficient over the resonance cell volume at all laser intensities, there is essentially no enhancement of RIN. For the intermediate values of τ_d , RIN enhancement is present at low laser intensities but is diminished at higher laser intensities. Specifically, for $\tau_d = 1.35$ cm and $\tau_d = 1.33$ cm the enhancement of RIN begins to decrease at $\log(I_{\text{inc}}) \approx 1.4$ and $\log(I_{\text{inc}}) \approx 2.2$, respectively. It is to be noted that these incident laser intensities correspond to the onset of fairly efficient optical pumping and to the creation of an optically thin vapor, according to the results presented in Fig. 2. The data of Fig. 4(b) therefore indicate that passage of laser light through a resonant atomic medium can increase the transmitted light's RIN by orders of magnitude if the resonant medium is optically thick. If the medium is optically thin, by virtue of low atomic density or efficient optical pumping, this significant enhancement of RIN does not occur. Additionally, inasmuch as the spectral density of the laser intensity noise was flat over the spectrum analyzer's 25-kHz bandwidth, the enhancement of RIN can be described as a white-noise process (at least at low Fourier frequencies).

5. THEORY OF RELATIVE INTENSITY NOISE IN AN OPTICALLY THICK, OPTICALLY PUMPED VAPOR

The present section has three goals. The first of these is to obtain a theory of PM-to-AM conversion in an optically thick vapor that predicts the orders-of-magnitude enhancement of laser RIN observed experimentally. It is to be noted that this degree of enhancement is not predicted by previous theory and is by no means an obvious extrapolation from previous theory owing to the nonlinear

relationship between $\chi''(z)$ and $E(z)$ in an optically thick vapor. The second goal is to use the theory to show that the enhancement of RIN disappears at high light intensities as a consequence of efficient optical pumping. The third goal is to use the theory to demonstrate that at low Fourier frequencies the laser intensity fluctuations generated by the PM-to-AM conversion process are white. Again, this is by no means an obvious deduction: The laser phase fluctuations are colored; they induce fluctuations in χ'' , and the fluctuations in χ'' have an exponential influence on the transmitted laser intensity.

Before we proceed to a discussion of the theory it is worth noting that there are several aspects to the problem that make its solution nontrivial. Because the phenomenon requires an optically thick vapor, the susceptibility $\chi''(r, z)$ (where z is the propagation distance into the vapor and r is a radial location) will depend on $E(r, z)$, which in turn depends on $\int \chi''(r, z') dz'$ ($0 \leq z' < z$). Thus the density matrix equations that describe the field-atom interaction must be solved numerically and the solution of $E(r, z)$ iterated through the vapor. Moreover, as optical pumping will have important consequences for the theory, the spatial distribution of the $|F = 2\rangle - |F = 1\rangle$ population imbalance must be included in the theory. (The spatial distribution of the population imbalance results from the diffusion of optically pumped atoms to the resonance cell walls, where wall collisions equalize the $F = 2$ and $F = 1$ populations.²⁷) Finally, to make contact with the experimental measurements it is necessary to solve for the spectral density of intensity fluctuations.

We obtain the system of equations that describes the fluctuations of the density matrix elements by decomposing the density matrix equations into two systems: one system for the density matrix mean values and another for the stochastic fluctuations. To obtain a time series for the transmitted laser intensity we solve the density matrix equations numerically, employing simulated stochastic variations of the laser field. We analyze the Allan variance of the time series to obtain the magnitude of laser RIN and its spectral characteristics.

As the problem is quite complicated, we invoke several approximations to develop a theory that highlights the physically relevant aspects of the phenomenon. Rather than considering the actual density matrix of ⁸⁷Rb, the theory considers a fictitious three-level atom. The theory is restricted to one spatial dimension and, rather than solving a system of partial differential equations to account for spatial diffusion, we employ a spatially varying relaxation rate in the density matrix equations. Finally, we ignore the influence of radiation trapping on the optical pumping process. Although the neglect of radiation trapping will not allow the theory to predict the sensitive alkali density dependence in the falloff of RIN with laser intensity, the theory should nonetheless be capable of predicting the correct magnitude of RIN as a consequence of efficient PM-to-AM conversion and the general falloff behavior as a consequence of optical pumping.

Defining σ_{ij} as the atomic density matrix elements of a three level system in the rotating frame, we can write the expectation value of atomic susceptibility as

$$\langle \chi(z) \rangle = N \langle \alpha(z) \rangle, \quad (7)$$

where N is the total number density of rubidium atoms in the vapor and α is the atomic polarizability. Note that α depends on z because it is a function of the applied electric field at position z .²⁸ We can write the polarizability in terms of the atomic density matrix elements by noting that the induced atomic dipole moment $\langle \mu \rangle$ equals $\langle \alpha \rangle E$, so

$$\langle \alpha'(z) \rangle = \frac{2\mu_{23}}{E(z)} \text{Re}[\sigma_{23}(z)], \quad (8)$$

$$\langle \alpha''(z) \rangle = \frac{2\mu_{23}}{E(z)} \text{Im}[\sigma_{23}(z)], \quad (9)$$

where α' and α'' refer to the real and the imaginary parts of the polarizability, respectively, and μ_{23} is the dipole matrix element connecting $|3\rangle$ and $|2\rangle$. For a small increment in the position, δz , the laser electric field can be expanded in a Taylor series about the position z by use of Eq. (2):

$$E(z + \delta z) = E(z) - \frac{8\pi^2 N \mu_{23}}{n^2 \lambda} \langle |\text{Im}[\sigma_{23}(z)]| \rangle_v \delta z, \quad (10)$$

where $\langle \dots \rangle_v$ implies a velocity average over the Maxwell-Boltzmann distribution. Computationally, we use the laser electric field amplitude at the position z to determine the density matrix elements $\sigma_{22}(z)$ and $\sigma_{23}(z)$ and then use Eq. (10) to determine the laser electric field amplitude in the neighboring region. Iterating this process from $z = 0$ to $z = L$, we determine the laser electric field amplitude, and hence the laser intensity, at the exit of the vapor for a given wave front of the incident field.

For the system of Fig. 1(b) the atomic density matrix equations at the spatial position z are

$$\dot{\sigma}_{11} = \frac{A}{2} \sigma_{33} + \gamma_{\text{hfs}}(\sigma_{22} - \sigma_{11}), \quad (11a)$$

$$\dot{\sigma}_{22} = -\frac{i\Omega}{2}(\sigma_{32} - \sigma_{23}) + \frac{A}{2} \sigma_{33} - \gamma_{\text{hfs}}(\sigma_{22} - \sigma_{11}), \quad (11b)$$

$$\dot{\sigma}_{33} = \frac{i\Omega}{2}(\sigma_{32} - \sigma_{23}) - A\sigma_{33}, \quad (11c)$$

$$\dot{\sigma}_{32} = i\Delta\sigma_{32} - \frac{i\Omega}{2}(\sigma_{22} - \sigma_{33}) - \left(\Gamma_c + \frac{A}{2}\right)\sigma_{32}. \quad (11d)$$

Here, Ω is the $|3\rangle \rightarrow |2\rangle$ Rabi frequency equal to $\mu_{23}E(z)/\hbar$, Δ is the laser detuning (i.e., $\Delta = \omega_0 + \delta\omega - \omega_{32}$), and Γ_c is the collisional dephasing rate of the optical transition. In the expression for the detuning, ω_0 is the average laser frequency and $\delta\omega$ is a mean-zero stochastic frequency fluctuation:

$$\langle \delta\omega(t)\delta\omega(t - \tau) \rangle = \gamma\beta \exp(-\beta|\tau|). \quad (12)$$

For single-mode lasers with nearly Lorentzian line shapes, 2γ is essentially the linewidth of the field (FWHM) and $\beta \gg \gamma$.²⁹

If Eq. (11c) is formally integrated, and only weak fields are considered such that the optical transition is not saturated, then

$$\sigma_{33}(t) \cong \frac{i\Omega}{2A}(\sigma_{32} - \sigma_{23}). \quad (13)$$

Moreover, it is to be noted that under these weak-field conditions $\sigma_{22} + \sigma_{11} \cong 1$. Thus, when u and v are defined as the real and the imaginary parts of σ_{32} , respectively, Eqs. (11) become

$$\dot{\sigma}_{22} = \frac{\Omega v}{2} - \gamma_{\text{hfs}}(2\sigma_{22} - 1), \quad (14a)$$

$$\dot{u} = -\left(\Gamma_c + \frac{A}{2}\right)u - \Delta v, \quad (14b)$$

$$\dot{v} = -\left(\Gamma_c + \frac{A}{2} + \frac{\Omega^2}{2A}\right)v + \Delta u - \frac{\Omega}{2}\sigma_{22}. \quad (14c)$$

As Eqs. (14) are to be solved under equilibrium conditions, we can let $\sigma_{22} = \Sigma + \delta_\sigma(t)$, $u = u_0 + \delta_u(t)$, and $v = v_0 + \delta_v(t)$, where Σ , u_0 , and v_0 are the mean, equilibrium values of the density matrix elements and $\delta_\sigma(t)$, $\delta_u(t)$, and $\delta_v(t)$ are mean-zero stochastic fluctuations of the density matrix elements. (In what follows, the explicit time dependence is dropped when these stochastic terms are written.) Zoller and Lambropoulos³⁰ have shown that in steady state

$$\dot{\Sigma} = 0 = \frac{\Omega}{2}v_0 - \gamma_{\text{hfs}}(2\Sigma - 1), \quad (15a)$$

$$\dot{u}_0 = 0 = -\left(\Gamma_c + \frac{A}{2}\right)u_0 - \gamma u_0 - (\omega_0 - \omega_{32})v_0, \quad (15b)$$

$$\dot{v}_0 = 0 = -\left(\Gamma_c + \frac{A}{2} + \frac{\Omega^2}{2A}\right)v_0 - \gamma v_0 + (\omega_0 - \omega_{32})u_0 - \frac{\Omega}{2}\Sigma, \quad (15c)$$

which are easily solved for the average density matrix elements. Then, combining Eqs. (15) and (14), we obtain a set of equations that describes the stochastic variations of the atomic density matrix elements:

$$\dot{\delta}_\sigma = \frac{\Omega(t)}{2}\delta_v - 2\gamma_{\text{hfs}}\delta_\sigma, \quad (16a)$$

$$\dot{\delta}_u = -\left(\Gamma_c + \frac{A}{2}\right)\delta_u + \gamma u_0 - [\omega_0 + \delta\omega(t) - \omega_{32}]\delta_v - \delta\omega(t)v_0, \quad (16b)$$

$$\dot{\delta}_v = -\left[\Gamma_c + \frac{A}{2} + \frac{\Omega^2(t)}{2A}\right]\delta_v + \gamma v_0 + [\omega_0 + \delta\omega(t) - \omega_{32}]\delta_u + \delta\omega(t)u_0 - \frac{\Omega(t)}{2}\delta_\sigma. \quad (16c)$$

Note that an explicit time dependence for the Rabi frequency has been included in Eqs. (16) to account for a laser's intrinsic intensity noise and the PM-to-AM conversion process. Specifically, we consider $\Omega(z = 0, t) = \Omega(0)[1 + x(t)]$,²⁹ where x is a mean-zero stochastic fluctuation that (for present purposes) is statistically independent of $\delta\omega(t)$ and where

$$\langle x(t)x(t-\tau) \rangle = \frac{\gamma}{\omega_1} \exp(-\omega_1|\tau|). \quad (17)$$

In Eq. (17), ω_1 is related to the laser's intrinsic RIN in a 1-Hz bandwidth: $\text{RIN} = 4\sqrt{\gamma}/\omega_1$.

Briefly, at various computational time steps, values for the stochastic laser electric field amplitude and frequency at $z = 0$ are determined by use of a methodology described in Ref. 29. The propagation of this wave front through the medium is then determined with the aid of Eqs. (10), (15), and (16). Equations (16) are solved at each position z by a fifth-order Runge-Kutta-Fehlberg method with adaptive step size,³¹ and the step size is restricted so it is always smaller than $0.1A^{-1}$ and $0.1\Gamma_c^{-1}$. Ten sets of density matrix equations are solved at each position z , corresponding to specific velocity subgroups. The attenuation coefficient (i.e., $\delta E/\delta z$) is averaged over the Doppler distribution by use of Gaussian quadrature³² and is then employed in Eq. (10) to propagate the laser electric field through the atomic vapor.³³ Moreover, to account for the slow diffusion of atoms to the resonance cell walls, where wall collisions equalize the $F = 2$ and $F = 1$ ground-state populations, γ_{hfs} is given a spatial dependence³⁴:

$$\gamma_{\text{hfs}} = \gamma_{\text{se}} + \gamma_{\text{bg}} + \frac{\pi^2 D}{4z^2}, \quad 0 \leq z \leq L/2, \quad (18a)$$

$$\gamma_{\text{hfs}} = \gamma_{\text{se}} + \gamma_{\text{bg}} + \frac{\pi^2 D}{4(L-z)^2}, \quad L/2 \leq z \leq L. \quad (18b)$$

Here γ_{se} and γ_{bg} are the relaxation rates that are due to spin-exchange and buffer-gas collisions, respectively, and D is the diffusion coefficient for rubidium atoms in the buffer gas. Although in all rigor a diffusion term should be added to the density matrix equations,¹⁵ this procedure captures the physical requirement on the $F = 2$ population that $\sigma_{22}(0) = \sigma_{22}(L) = 0.5$. The intensity of the laser at the exit of the medium is averaged over a time interval equal to the smaller of either A^{-1} or Γ_c^{-1} and then subjected to statistical analysis.

An example of the computed laser intensity variation at the exit of a 3-cm-long resonance cell at 50 °C is shown in Fig. 5(a). For this example the laser had a linewidth (2γ) of 1 GHz ($\beta = 2$ GHz) and an intrinsic RIN of 10^{-10} . Thus the stochastic variations illustrated in the figure are solely the result of laser propagation through the resonant medium. Moreover, the incident laser intensity was chosen as $1 \mu\text{W}/\text{cm}^2$ to eliminate optical pumping effects. To compute the transmitted laser intensity RIN, time series such as that of Fig. 5(a) were used to compute the Allan standard deviation of the transmitted laser intensity noise, $\sigma_I(\tau)$.^{35,36} This computation is shown in Fig. 5(b) for the data of Fig. 5(a), where the square-root dependence of $\sigma_I(\tau)$ on averaging time τ indicates that the transmitted laser intensity noise is white. [In all the calculations, $\sigma_I(\tau)$ was inversely proportional to $\sqrt{\tau}$.] For white noise, $\sigma_I^2(\tau) = S_I/2\tau$, where S_I is the one-sided white-noise spectral density of the transmitted laser intensity fluctuations. Consequently $\sigma_I(\tau)$ at $\tau = 1$ s (determined by a linear least-squares fit) provides

an unambiguous measure of the laser intensity noise in a 1-Hz bandwidth and hence of the RIN.

Figure 6 shows the results of the computations for the parameters listed in Table 1. (Resonance cell temperature essentially determined the alkali vapor density.³⁹) As in the experimental case, the optical depth of the vapor was determined by the ratio of the average incident laser intensity to the average transmitted laser intensity. As was observed in the experiment, for an optical depth of ~ 1.5 cm there is roughly a 2-orders-of-magnitude increase in the transmitted laser intensity RIN at low light intensities, but at high light intensities where optical pumping is efficient the transmitted laser intensity RIN drops to its intrinsic value. For the larger optical depth of 2.1 cm the enhancement of RIN at low light intensities is smaller, and the falloff to the intrinsic RIN occurs at lower light intensities.

The major discrepancy between the present theory and experiment is the sensitivity of the falloff in RIN to changes in the alkali density. Experimentally, a change in the optical depth of 0.02 cm yielded a dramatic change in the intensity where the falloff from enhanced RIN to

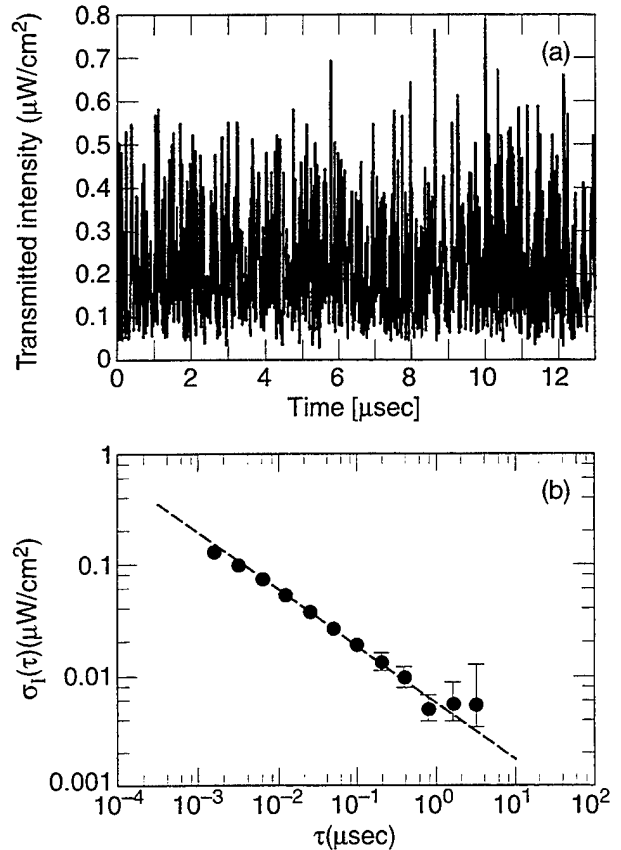


Fig. 5. (a) Example of computational laser transmitted intensity variations through 3 cm of a 50 °C vapor for a laser with a 1-GHz linewidth and a RIN of 10^{-10} . The incident laser intensity was $1 \mu\text{W}/\text{cm}^2$, and the average transmitted laser intensity was $0.22 \mu\text{W}/\text{cm}^2$. (b) Log-log plot of the Allan standard deviation $\sigma_I(\tau)$ versus averaging time τ . The dashed line is a linear least-squares fit to the data. The slope of 0.5 for the fit indicates that the laser intensity fluctuations are white, and the intercept $\{\log[\tau(s)] = 0\}$ is a measure of the intensity fluctuations' spectral density.

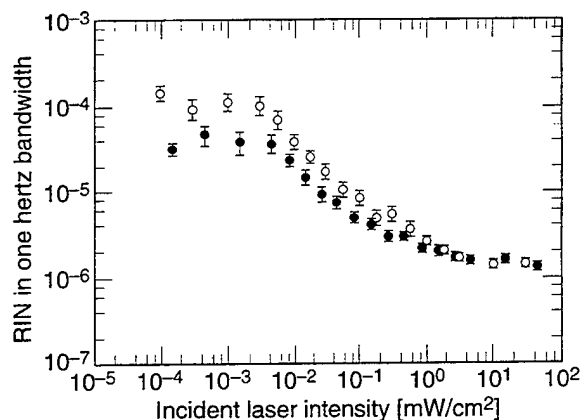


Fig. 6. Computational results for the RIN of laser light transmitted through a resonant rubidium vapor: open circles, $\tau_d = 1.5$ cm; filled circles, $\tau_d = 2.1$ cm. For $\tau_d = 1.5$ cm the resonance cell temperature was 40 °C, and for $\tau_d = 2.1$ cm the resonance cell temperature was 35 °C. Error bars in the figure are semiquantitative and arise from an uncertainty in estimating the intercept $\{\log[\tau(s)] = 0\}$ of the log-log Allan standard deviation plots.

Table 1. Parameters Used in the Computation of the Data Presented in Fig. 6

Parameter	Value
Resonance cell length, L	3 cm
Collisional dephasing rate, Γ_c	100 MHz
Rb-Rb spin-exchange cross section ^a	1.9×10^{-14} cm ²
Rb-N ₂ hyperfine relaxation cross section ^b	8.3×10^{-23} cm ²
Rb diffusion coefficient in N ₂ (i.e., D_0) ^b	0.16 cm ² /s
N ₂ pressure	10 Torr
Resonance cell temperature	35 and 40 °C
Laser linewidth, 2γ	50 MHz
β	1 GHz
Laser's intrinsic RIN	10^{-6}

^a Ref. 37.

^b Ref. 38.

intrinsic RIN occurred. Theoretically, increasing the optical depth by 40% changed the intensity where this fall-off occurred by much less than an order of magnitude. Because it has been argued that optical pumping is strongly influenced by radiation trapping in optically thick vapors, radiation trapping must consequently play an important role in the PM-to-AM conversion process. Moreover, radiation trapping quite likely influences the atomic coherence (regardless of optical pumping) and hence the stochastic fluctuations of χ'' . Nonetheless, a consideration of radiation trapping does not appear to be requisite to a semiquantitative description of the PM-to-AM conversion process in optically thick vapors, because the present theory without radiation trapping has demonstrated (1) the experimentally observed orders-of-magnitude enhancement of laser RIN, (2) that the enhancement of laser RIN is eliminated at high light intensities where optical pumping is efficient, and (3) that at low Fourier frequencies the laser intensity fluctuations are white.

6. SUMMARY

Here it has been shown that laser intensity noise can be increased by orders of magnitude when it propagates through an optically thick resonant medium. The effect arises because laser phase fluctuations produce variations in the atomic coherence, which essentially manifest themselves as noise in the atomic absorption cross section. For an optically thick vapor the transmitted laser intensity has an exponential dependence on the absorption cross section, so there is a dramatic effect on the transmitted laser light's RIN.

As was alluded to in Section 1, the conversion of PM to AM in an atomic vapor has important technological implications. For several years now, metrological laboratories around the world have been pursuing a goal of improved atomic clock performance by using diode lasers to optically pump an alkali vapor.⁴⁰ In these devices the laser light transmitted through the vapor generates the atomic clock signal. Present-day devices use rf-discharge lamps to generate the atomic signal, and because of their relatively inefficient optical pumping the atomic clock's signal is small.⁷ As might be expected, the stability of the atomic clock is directly related to the signal-to-noise ratio, and the largest signals are typically obtained with optically thick vapors and diode-laser optical pumping. However, the optically thick vapors also dramatically increase the signal's noise level in the case of diode-laser optical pumping because of the PM-to-AM conversion process discussed here.⁴¹ In fact, we find that under certain conditions the increased noise level that is due to PM-to-AM conversion is larger than the increased signal level that comes from efficient diode-laser optical pumping.⁴² Consequently, substituting a diode laser for a rf-discharge lamp in these atomic clocks can sometimes degrade performance. Mitigating the influence of this noise process to achieve the full potential of diode-laser optical pumping in atomic clocks will require a better understanding of the role of laser line shape, optical density, and radiation trapping in the PM-to-AM conversion process.

REFERENCES AND NOTES

1. T. Yabuzaki, T. Mitsui, and U. Tanaka, "New type of high-resolution spectroscopy with a diode laser," *Phys. Rev. Lett.* **67**, 2453 (1991).
2. R. Walser and P. Zoller, "Laser-noise-induced polarization fluctuations as a spectroscopic tool," *Phys. Rev. A* **49**, 5067 (1994).

3. D. H. McIntyre, C. E. Fairchild, J. Cooper, and R. Walser, "Diode-laser noise spectroscopy of rubidium," *Opt. Lett.* **18**, 1816 (1993).
4. R. J. McLean, P. Hannaford, C. E. Fairchild, and P. L. Dyson, "Tunable diode-laser heterodyne spectroscopy of atmospheric oxygen," *Opt. Lett.* **18**, 1675 (1993).
5. K. V. Vasavada, G. Vemuri, and G. S. Agarwal, "Diode-laser-noise-based spectroscopy of allowed and crossover resonances," *Phys. Rev. A* **52**, 4159 (1995).
6. R. Walser, J. Cooper, and P. Zoller, "Saturated absorption spectroscopy using diode-laser phase noise," *Phys. Rev. A* **50**, 4303 (1994).
7. J. C. Camparo and R. P. Frueholz, "A nonempirical model of the gas-cell atomic frequency standard," *J. Appl. Phys.* **59**, 301 (1986); "Fundamental stability limits for the diode-laser-pumped rubidium atomic frequency standard," *J. Appl. Phys.* **59**, 3313 (1986).
8. See, for example, T. G. Vold, F. J. Raab, B. Heckel, and E. N. Fortson, "Search for a permanent electric dipole moment on the ^{129}Xe atom," *Phys. Rev. Lett.* **52**, 2229 (1984); S. Appelt, G. Wackerle, M. Mehring, "A magnetic resonance study of non-adiabatic evolution of spin quantum numbers," *Z. Phys. D* **34**, 75 (1995).
9. See, for example, M. H. Anderson, R. D. Jones, J. Cooper, S. J. Smith, D. S. Elliot, H. Ritsch, and P. Zoller, "Variance and spectra of fluorescence-intensity fluctuations from two-level atoms in a phase-diffusing field," *Phys. Rev. A* **42**, 6690 (1990), and references therein.
10. P. Meystre and M. Sargent III, *Elements of Quantum Optics* (Springer-Verlag, Berlin, 1991), Chap. 1.
11. Note that $(1/\nu)(\partial E/\partial t) \approx (\delta t_p/L)(E/\tau_c)$, where L is the length of the medium, δt_p is the propagation time of a wave front through the medium, and τ_c is the correlation time of the field's stochastic variations. For a medium with a length of a few centimeters, $\delta t_p \sim 10^{-10}$ s, whereas for the lasers of interest in our study $\tau_c \sim 10^{-8}$ s. Thus the temporal variation of the electric field will be roughly 2 orders of magnitude smaller than the spatial variation for an optically thick medium where $(\partial E/\partial z) \approx E/L$.
12. It should be noted that in addition to Eq. (1) there is a propagation equation for the phase of the field: $\partial \phi/\partial z + (1/\nu)(\partial \phi/\partial t) = -[(2\pi k/n^2)\chi'(z, E)]$. Inasmuch as the laser's phase noise yields fluctuations in both χ' and χ'' , the optical field's phase fluctuations grow in a complicated fashion as the field propagates through the medium. The greater degree of phase noise further enhances the fluctuations of χ'' , which in turn results in larger variations of the laser's transmitted intensity. However, because χ' is proportional to the real part of the atomic coherence, which is generally small unless the laser has frequency excursions of the order of the optical homogeneous linewidth, it seems reasonable to ignore this additional source of laser phase noise in the PM-to-AM conversion process associated with the present experimental conditions: laser linewidth, ≈ 60 MHz and atomic homogeneous linewidth, ≈ 200 MHz. It is worth noting, though, that there will be experimental conditions in which this additional phase noise could be an important aspect of the PM-to-AM conversion process.
13. The acronyms TJS and CSP stand for transverse junction stripe and channeled substrate planar, respectively, and refer to the physical construction of the diode laser. See D. Botez, "Single-mode AlGaAs diode lasers," *J. Opt. Commun.* **1**, 42 (1980) for a more detailed discussion.
14. J. C. Camparo, "The diode laser in atomic physics," *Contemp. Phys.* **26**, 443 (1985); C. E. Wieman and L. Hollberg, "Using diode lasers for atomic physics," *Rev. Sci. Instrum.* **62**, 1 (1991).
15. W. Happer, "Optical pumping," *Rev. Mod. Phys.* **44**, 169 (1972).
16. V. N. Belov, "Application of the magnetic-scanning method to the measurement of the broadening and shift constants of the rubidium D_2 line (780.0 nm) by foreign gases," *Opt. Spectrosc. (USSR)* **51**, 22 (1981).
17. P. Minguzzi and A. Di Lieto, "Simple Padé approximations for the width of a Voigt profile," *J. Mol. Spectrosc.* **109**, 388 (1985).
18. I. Botev, "A new conception of Bouguer-Lambert-Beer's law," *Fresenius J. Anal. Chem.* **297**, 419 (1979).
19. N. D. Bhaskar, M. Hou, B. Suleman, and W. Happer, "Propagating, optical-pumping wave fronts," *Phys. Rev. Lett.* **43**, 519 (1979).
20. A. C. G. Mitchell and M. W. Zemansky, *Resonance Radiation and Excited Atoms* (Cambridge U. Press, London, 1971), Chap. IV.
21. L. Krause, "Sensitized fluorescence and quenching," in *The Excited State in Chemical Physics*, J. W. McGowan, ed. (Wiley, New York, 1975), Vol. XXVIII, Chap. 4.
22. See J. C. Camparo and S. B. Delcamp, "Optical pumping with laser-induced-fluorescence," *Opt. Commun.* **120**, 257 (1995), and the discussion regarding C. H. Volk, J. C. Camparo, and R. P. Frueholz, "Investigations of laser pumped gas cell atomic frequency standard," in *Proceedings of the 13th Annual Precise Time and Time Interval (PTTI) Applications and Planning Meeting* (U.S. Naval Observatory, Washington, D.C., 1981), pp. 631-640.
23. See, for example, A. F. Molisch, W. Schupita, B. P. Oehry, B. Sumetsberger, and G. Magerl, "Modeling and efficient computation of nonlinear radiation trapping in three-level atomic vapors," *Phys. Rev. A* **51**, 3576 (1995).
24. D. Tupa, L. W. Anderson, D. L. Huber, and J. E. Lawler, "Effect of radiation trapping on the polarization of an optically pumped alkali-metal vapor," *Phys. Rev. A* **33**, 1045 (1986); D. Tupa and L. W. Anderson, "Effect of radiation trapping on the polarization of an optically pumped alkali-metal vapor in a weak magnetic field," *Phys. Rev. A* **36**, 2142 (1987).
25. Y. Yamamoto, S. Saito, and T. Mukai, "AM and FM quantum noise in semiconductor lasers. II. Comparison of theoretical and experimental results for AlGaAs lasers," *IEEE J. Quantum Electron.* **QE-19**, 47 (1983).
26. H. Tsuchida and T. Tako, "Relation between frequency and intensity stabilities in AlGaAs semiconductor laser," *Jpn. J. Appl. Phys.* **22**, 1152 (1983).
27. P. Minguzzi, F. Strumia, and P. Violino, "Temperature effects in the relaxation of optically oriented alkali vapors," *Nuovo Cimento* **46B**, 145 (1966).
28. Because of the presence of the buffer gas, the atoms are essentially frozen in place. Thus individual atoms experience local values of the electric field amplitude rather than averaging the electric field amplitude over the resonance cell volume. See J. C. Camparo, R. P. Frueholz, and C. H. Volk, "Inhomogeneous light shift in alkali-metal atoms," *Phys. Rev. A* **27**, 1914 (1983); R. P. Frueholz and J. C. Camparo, "Microwave field strength measurement in a rubidium clock cavity via adiabatic rapid passage," *J. Appl. Phys.* **57**, 704 (1985).
29. J. C. Camparo and P. Lambropoulos, "Monte Carlo simulation of field fluctuations in strongly driven resonant transitions," *Phys. Rev. A* **47**, 480 (1993).
30. P. Zoller and P. Lambropoulos, "Non-Lorentzian laser line-shapes in intense field-atom interaction," *J. Phys. B* **12**, L547 (1979).
31. W. Cheney and D. Kincaid, *Numerical Mathematics and Computing* (Brooks Cole, Monterey, Calif., 1985); W. H. Press and S. A. Teukolsky, "Adaptive stepsize Runge-Kutta integration," *Comput. Phys.* **6**, 188 (1992).
32. R. H. Pennington, *Introductory Computer Methods and Numerical Analysis* (Macmillan, London, 1970).
33. Note that with 10 Torr of N_2 the time between velocity-changing collisions is $\sim 10^{-7}$ s, based on a gas kinetic cross section for velocity-changing collisions, whereas the propagation time of a wave front through a 3-cm medium is $\sim 10^{-10}$ s. Thus, on the time scale of a wave front's propagation through the medium, each atom has a specific, essentially constant, velocity.
34. F. A. Franz, "Relaxation at cell walls in optical pumping experiments," *Phys. Rev. A* **6**, 1921 (1972).
35. The Allan standard deviation, or Allan variance, is a statistic that is typically employed to describe precise frequency

standards; it has the attractive property that it converges for certain nonstationary noise processes. Essentially, a fluctuating parameter is averaged over some time τ , and differences between neighboring averages are computed. The Allan variance is the variance associated with these differences. In the present work we take advantage of the ease with which the Allan variance may be computed and its well-known relationship to the noise process's spectral density.

36. J. Rutman, "Characterization of phase and frequency instabilities in precision frequency sources: fifteen years of progress," *Proc. IEEE* **66**, 1048 (1978); J. A. Barnes, A. R. Chi, L. S. Cutler, D. J. Healey, D. B. Leeson, T. E. McGun-
ingal, J. A. Mullen, Jr., W. L. Smith, R. L. Sydnor, R. F. C. Vessot, and G. M. R. Winkler, "Characterization of frequency stability," *IEEE Trans Instrum. Meas.* **IM-20**, 105 (1971).
37. N. W. Ressler, R. H. Sands, and T. E. Stark, "Measurement of spin-exchange cross sections for Cs^{133} , Rb^{87} , Rb^{85} , K^{39} , and Na^{23} ," *Phys. Rev.* **184**, 102 (1969).
38. F. A. Franz and C. Volk, "Spin relaxation of rubidium atoms in sudden and quasimolecular collisions with light-noble-gas atoms," *Phys. Rev. A* **14**, 1711 (1976).
39. T. J. Killian, "Thermionic phenomena caused by vapors of rubidium and potassium," *Phys. Rev.* **27**, 578 (1926).
40. C. Szekely, F. L. Walls, J. P. Lowe, R. E. Drullinger, and A. Novick, "Reducing local oscillator phase noise limitations on the frequency stability of passive frequency standards: tests of a new concept," *IEEE Trans. Ultrason. Ferroelectr. Freq. Control* **41**, 518 (1994); Y. Saburi, Y. Koga, S. Kinugawa, T. Imamura, H. Suga, and Y. Ohuchi, "Short-term stability of laser-pumped rubidium gas cell frequency standard," *Electron. Lett.* **30**, 633 (1994); P. J. Chantry, I. Liberman, W. R. Verbanets, C. F. Petronio, R. L. Cather, and W. D. Partlow, "Miniature laser-pumped cesium cell atomic clock oscillator," in *Proceedings of the 1996 IEEE Frequency Control Symposium* (IEEE Press, Piscataway, N.J., 1996), pp. 1002-1010; L. A. Budkin, V. L. Velichanski, A. S. Zibrov, A. A. Lyalyaskin, M. N. Penenkov, and A. I. Pikhteleev, "Double radio-optical resonance in alkali metal vapors subjected to laser excitation" *Sov. J. Quantum Electron.* **20**, 301 (1990); M. Hashimoto and M. Ohtsu, "Experiments on a semiconductor laser pumped rubidium atomic clock," *IEEE J. Quantum Electron.* **QE-23**, 446 (1987).
41. G. Milette, J. Q. Deng, F. L. Walls, J. P. Lowe, and R. E. Drullinger, "Recent progress in laser-pumped rubidium gas-cell frequency standard," in *Proceedings of the 1996 IEEE International Frequency Control Symposium* (IEEE Press, Piscataway, N.J., 1996), pp. 1066-1072.
42. J. C. Camparo and W. F. Buell, "Laser PM to AM conversion in atomic vapors and short term clock stability," in *Proceedings of the 1997 IEEE International Frequency Control Symposium* (IEEE Press, Piscataway, N.J., 1997), pp. 253-258.